TECHNICAL NOTE

Effect of Suspended Sediment on Acoustic Detection Using Reverberation

AUTHORS

Peter C. Chu
Michael Cornelius
Naval Ocean Analysis and Prediction Laboratory
Department of Oceanography
Naval Postgraduate School

Mel Wagstaff
Naval Oceanographic Office
Stennis Space Center

ABSTRACT

Sonar operates by ensonifying a broad swath of the seabed using a line array of acoustic projectors with acoustic backscattering from the ensonified sediment. The suspended sediment layer affects the sonar imagery through the volume scattering strength. Understanding the acoustic characteristics of the suspended sediment layer can aid the Navy in detecting sea mines with sonar imagery. In this study, the Navy's Comprehensive Acoustic Simulation System is used to investigate such an effect. A range of critical values of volume scattering strength for buried object detection is found through repeated model simulations.

INTRODUCTION

coustic detection of undersea objects is difficult due to the uncertain environment (Chu et al., 2002, 2004) and even more difficult when the objects are buried in the seabed. First, sediments generate high backscattering noise due to heterogeneous scatters within the sediments clouding the object.

Second, the acoustic wave attenuation in sediments is much higher than in water. Acoustic shadows make the buried targets absent in the sonar images due to diffraction around the target, transmission through the target and relatively high acoustic noise due to backscattering from sediments surrounding the target. Classification of buried targets is also more difficult since there are no shadows, and the images do not contain much information about target shape since scattering from oblique target surfaces is not detectable.

Acoustic images of buried targets primarily consist of echoes from the target surfaces that are normal to the incident acoustic ray path. Target surfaces with an oblique aspect to the incident ray path will backscatter much less energy at the lower operating frequencies of sub-bottom profilers since the acoustic wavelength is much longer than the surface roughness of most targets of interest.

The suspended sediment layer occupies the lower water column. Presence of the suspended sediments creates a volume scattering layer which affects acoustic detection. Understanding the acoustic effects of the suspended sediment layer leads to the development of acoustic sensors with capability to scan the seafloor and to detect ordnance such as sea mines.

2. Comprehensive Acoustic Simulation System

Sonar equations provide guidelines for system design (Urick, 1983). The governing equation for beam patterns with dominating volume reverberation is given by

$$SL - TL_i - TL_r + TS - RL = SNR \quad (1)$$

where SL is the source level; TL_i is the transmission loss of the incident wave; TL_r is the transmission loss of the reflected echo; TS is target strength; RL is the reverberation level of sediments; SNR is the signal-to-noise ratio of the sonar data. The transmission losses of the incident and reflected waves, TL_i and TL_r, account for spherical loss (such as spherical spreading), acoustic attenuation, and boundary loss.

Volume reverberation depends on the physical properties of the water column. With the presence of a suspended sediment layer, large quantities of sediment remain in the water column and significantly affect the acoustic transmission in the water. The denser the suspended sediment layer is, the harder it would be for sonar to penetrate through the water. Moreover, suspended bottom sediment layer increases the density of the lower water column and in turn changes the sound velocity profile and prevents acoustic energy from reaching a possible buried object.

Reverberation can be used to represent the effects of a suspended sediment layer on acoustic detection. The differential form of the reverberation can be obtained from integration over the ensonified area (Keenan, 2000),

$$d(RL) = SL + 10 \log (SA) + SS - TL_t - TL_f + BP_t + BP_r \quad (2)$$

where SA is the scattering area; SS is the scattering strength per unit area; TL_t is the transmission loss to scatterer; TL_f is the transmission loss from scatterer; BP_t is the beam pattern to scatterer; and BP_f is the beam pattern from scatterer. The most important design criterion for detecting mine-like objects is to maximize the SNR, the target echo to scattering noise ratio in decibels.

The Comprehensive Acoustic Simulation System (CASS) is the Navy's standard model for acoustic and sonar analysis. It incorporates the Gaussian Ray Bundle (GRAB) eigenray modes to predict range-dependent acoustic propagation in the 150 Hz to 100 kHz frequency band (Keenan et al., 1996; Keenan and Weinberg, 2001).

CASS contains several equations for sound speed conversions. The current OAML approved Sound Speed Algorithm (Chen and Millero, 1977; Millero and Li, 1994) has been incorporated into CASS. The Chen-Millero-Li equations compute sound speed based on depth, temperature, and salinity. The Chen-Millero-Li, Wilson (1969), and Leroy (1969) equations are all very close in the salinity range 30 ppt to 40 ppt. For lower salinities the Chen-Millero-Li equation should be used. Near shore off the coast of Louisiana may have salinity variability especially near the Mississippi Delta. Thus, the Chen-Millero-Li equations are used in this study.

CASS simulates the sonar performance reasonably well in the littoral zone with given environmental input data, such as bottom type, sound speed profile and wind speed and accurate tilt angle of the sound source (Chu et al., 2002, 2005). CASS successfully modeled torpedo acoustic performance in shallow water exercises off the coast of Southern California and Cape Cod. Recently, CASS was used to simulate mine warfare systems performance in the fleet (Keenan et al., 1996), and for AN/SQQ-32 mine hunting detection and classification sonar.

CASS calculates the reverberation in nested do loops, seven deep. Reverberation is a function of time and the inner loop collected all the reverberation contributions over the user-requested sampling times. There are two loops on eigenray paths, one for the paths connecting the transmitter to the scattering cell and the other for the paths connecting the scattering cell to the receiver. Since the reverberation is calculated in the time domain and there may be contributions in the same time bin from different ranges, the next loop increments the range. CASS combines the five possible eigenray paths at each range step and decides if the ray paths contribute to the reverberation time bin (Keenan, 2000).

Test rays are sorted into families of comparable numbers of turning points and boundary interactions. Ray properties are then power averaged for each ray family to produce a representative eigenray of that family. Target echo level and reverberation level are computed separately, and subtracted to get the signal-noise ratio in the absence of additive ambient noise—noise level is typically power summed with the reverberation level for total interference. A detection threshold is applied to compute SE, and then the peak signal is used to determine *SNR* (Figure 1).

3. Environmental and Acoustic Parameters

A nearshore location with silty clay bottom on the Louisiana shelf is selected. Horizontal extension of the area is 50 m × 60 m. Total depth including water and sediment is around 100 m. A hydrographic survey was conducted in the area (Cornelius, 2004). The sound speed increases a little from 1520 m s^{-1} near the ocean surface to 35 m depth, and reduces drastically to 1510.5 m s^{-1} at 55 m depth. Below 55 m depth, the sound speed decreases slightly with depth and reaches 1510 m s^{-1} at 100 m.

Suppose the sonar is towed at a depth of 30.4 m with a source level of 240 dB. The water depth in the area varies from 77 to 95 m. The extent of the image is approximately 60 m in the *y*-direction and 50 m in the *x*-direction. The grain size index for a silty clay bottom is 8 from the Naval Oceanographic Office's standard. This parameter is related to specific geoacoustic parameters of bottom reflection (APL-UW, 1994). The bottom reflection effects are modeled using the Rayleigh model.

The water column is assumed to be relatively clear above 77 m depth with a volume scattering strength of -95 dB. The source of the water column scattering strength is extracted from a volume scattering strength database (CNMOC, 2004). A suspended sediment layer is present below 77 m depth characterized by a different scattering strength (-65 dB). The source level is 240 dB. The sonar frequency is 100 kHz. The pulse length is 0.001 seconds. The time increment for modeling should not exceed one half of the pulse length to achieve proper resolution of each time step. Since the total distance traveled from the sonar to the end of the image is approximately 50 m, the total reverberation time is only 0.12 seconds. The maximum number of bottom and surface reflections is set at 30 to allow interference with reflected eigenrays.

FIGURE 1

Steps taken to create a total reverberation image from CASS, compared to the side scan sonar image.

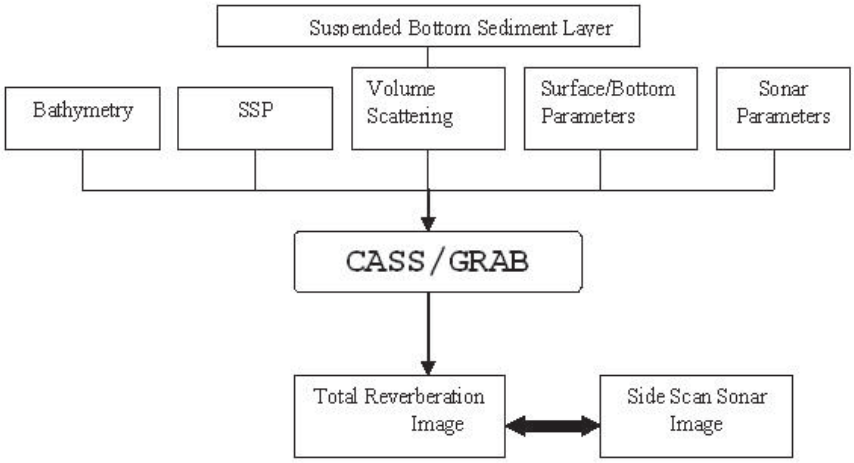

Test rays are sorted into families of comparable numbers of turning points and boundary interactions. Target echo level and reverberation level are typically computed separately, and then subtracted to get the signal-noise ratio. In the absence of additive ambient noise, the signal-noise ratio is typically power summed with the reverberation level to calculate total interference. A detection threshold is applied to compute SE, and then the peak signal is used to determine *SNR* (Figure 1).

4. Mine-Like Object

Let a hollow mine-like steel object (8 m × 5 m × 2 m) be placed near the center of the area with a height of 2 m. For the object, the grain size index is changed to -9 (clay) and the target strength is set as -35 dB. The bathymetry is also changed to represent the existence of the object. The water depth is kept the same (87 m) in the vicinity of the object, and changed into 85 m over the object (Figure 2).

CASS is integrated with the sonar parameters, sound speed profile (SSP), bottom type, bathymetry, and the scattering characteristics. The model output of the seafloor reverberation is used to represent the model generated sonar imagery (MGSI). An increase of the volume scattering strength in the lower water column reflects the presence of the suspended sediment layer. Clearly, the object is visible in the reverberation imagery. Since MGSI (Figure 3) is a replica of the sonar image, the effect of suspended sediment on acoustic detection may be studied using MGSI.

5. Effect of Suspended Sediment

Suspended sediment increases the volume scattering strength. To simulate its effect, the volume scattering strength is increased by an increment of 5 dB from the value of -65 dB below 78 m depth while keeping the volume scattering strength constant (-95 dB) above 78 m depth, and CASS is integrated with increasing the value of the volume scattering strength to investigate the effect of the suspended sediment on the object detection.

FIGURE 2
Bathymetry with mine-like object.

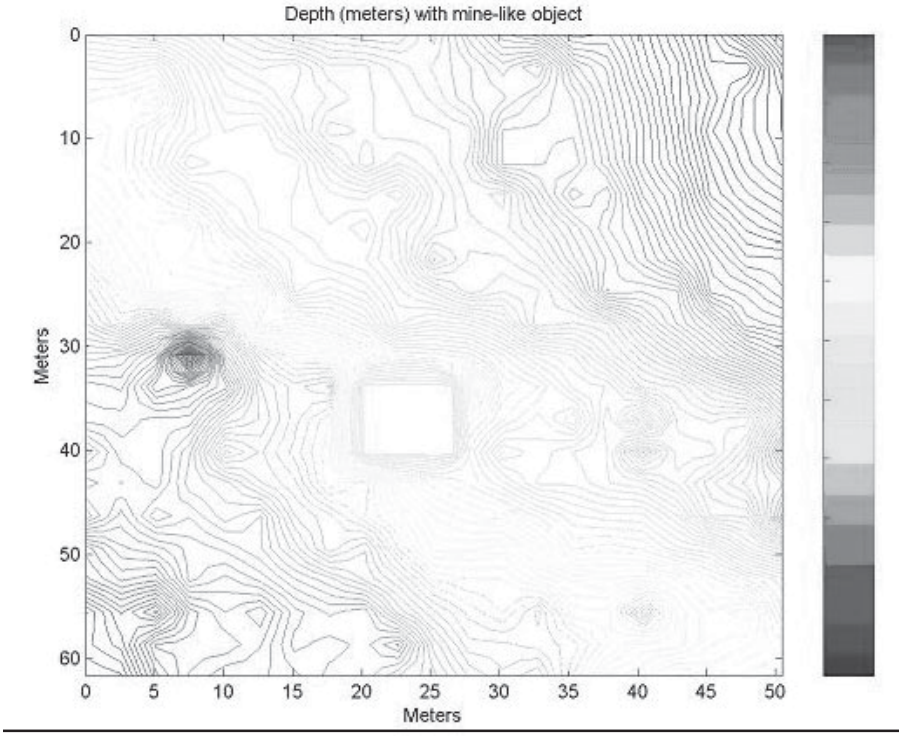

FIGURE 3
Bottom reverberation with mine-like object inserted. Here, the horizontal-axis is cross track indices represented by time and the vertical-axis is along track indices represented by distance.

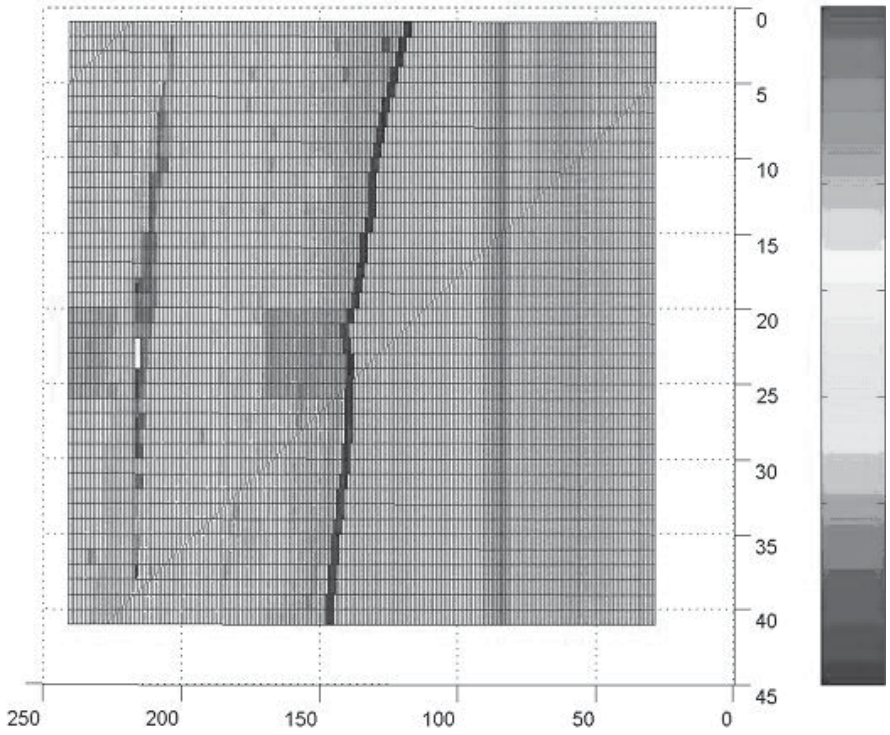

The following procedure is used to determine the criterion of the volume scattering strength for the object absent from MGSI. If the simulated mine-like object is still visible in MGSI after increasing the volume scattering, the simulated suspended sediment layer is not strong enough to represent a layer that would prevent a mine-like object from sonar detection. So the volume scattering strength is increased further. This procedure is performed until the mine-like object is no longer visible. During the simulation, the water column is assumed to be relatively clear above 77 m depth, with an initial suspended sediment layer characterized by a slightly stronger scattering strength below 78 m.

Sediment in the water column would increase the volume scattering and ultimately the volume reverberation. For MGSI with an object, a critical value of the volume scattering strength can be determined below 78 m depth to render the mine-like object undetectable. Volume attenuation and changes in the sound velocity profile will also have an effect, but they are not addressed in this work.

As the volume scattering strength of the sediment layer (below 78 m depth) increases to a value of -30 dB, the object becomes nearly undetectable. The CASS modeling continues with the increase of a smaller increment of 1 dB. The mine-like object is completely obscured (Figure 4) by the suspended sediment layer at a value of -22 dB (below 78 m depth), which is taken as the threshold.

This threshold (-22 dB) is large compared to existing observational data. For example, Kringel et al. (2003) measure the acoustic volume scattering strength in West Sound, Orcas Island, Washington, using the benthic acoustic monitoring system. It is a bottom-mounted, radially scanning sonar designed to record high-frequency scattering from the seafloor. The acoustic volume scattering strength is measured from 22 m of water column with 0.5 m vertical and 2 min temporal resolution. Their measurement shows that the volume backscattering strength varies between -75 dB to -25 dB. This indicates that the threshold (-22 dB) is in the high end, which implies that high suspended sediment density is needed to completely block the mine-like object from acoustic detection.

6. Conclusions

(1) CASS is used to investigate the effect of suspended sediment on detecting a mine-like object in the silty clay bottom at the Louisiana shelf with water depth around 100 m. Hydrographic and meteorological surveys were conducted. The environmental data (wind and SSP) are taken as the input into CASS to simulate the sonar image with a mine-like object present through its reverberation characteristics.

(2) A threshold of volume scattering strength (-22 dB) for the mine-like object detection is found through repeated model simulations. When the volume scattering strength increases to the threshold, the mine-like object is acoustically undetectable. It is noted that this threshold is very large and valid only for this case and that the purpose of this study is to show the methodology rather than to provide an accurate threshold.

(3) While CASS is useful, several shortfalls remain in this study. First, the process by which the environment and the object are modeled is cumbersome. Second, the appropriate volume scattering strength for the buried object should be given. A thorough study is suggested on the relationship between the suspended sediment layer density and type (e.g., sand, silt or clay), particle density in the layer, associated volume scattering strength and attenuation, and changes in the sound speed profile.

Acknowledgments

The Office of Naval Research, Naval Oceanographic Office, and the Naval Postgraduate School supported this study.

FIGURE 4

Reverberation plot of bottom with mine object inserted. The horizontal axis is cross track indices represented by time and the vertical axis is along track indices represented by distance with mine object inserted and suspended sediment layer with -22 dB volume scattering strength.

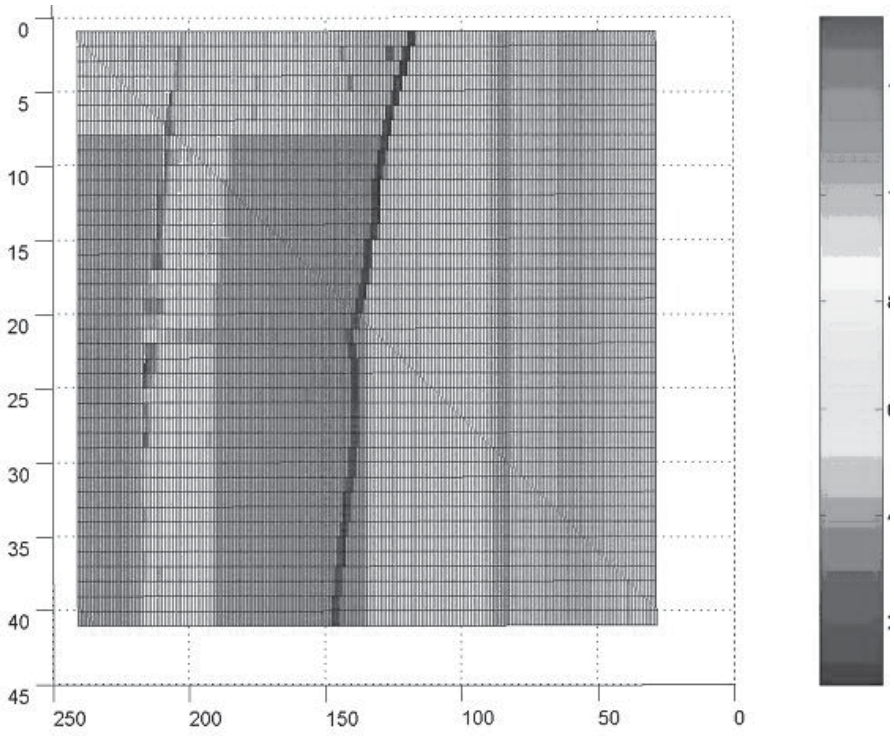

References

APL-UW. 1994. High-Frequency Ocean Environmental Acoustics Models Handbook. *APL-UW TR 9407*, Applied Physics Laboratory, University of Washington, Seattle, 210 p.

Chen, C. T. and Millero, F. J. 1977. Speed of Sound in Seawater at High Pressures. J Acoust Soc Am. 62(5):1129-1135.

Chu, P.C., C.J. Cintron, S.D. Haeger, D. Schneider, R.E. Keenan and D.N. Fox. 2002. Yellow Sea acoustic uncertainty caused by hydrographic data errors. In: Impact of Littoral Environment Variability on Acoustic Prediction and Sonar Performance, eds. N.G. Pace and F. B. Jensen. pp. 563-570. Boston: Kluwar Academic Publishers.

Chu, P.C., M.D. Perry, E.L. Gottshall, and D.S. Cwalina. 2004. Satellite data assimilation for improvement of Naval undersea capability. Mar Technol Soc J. 38(1):12-23.

Chu, P.C. and N.A. Vares. 2005. Variability in shallow sea acoustic detection due to environmental uncertainty, U.S. Navy Journal of Undersea Acoustics, in press.

Commander Naval Meteorology and Oceanography Command (CNMOC). 2004. Oceanography and Meteorology Master Library, Stennis Space Center, MS.

Cornelius, M. 2004. Effects of a Suspended Sediment Layer on Acoustic Imagery. MS Thesis in Meteorology and Physical Oceanography, Naval Postgraduate School, Monterey, CA, 48 pp.

Keenan, R. E., H. Weinberg, F.E. Aidala. 1996. Modeling Cape Cod site C and site D torpedo reverberation data with CASS. Naval Undersea Warfare Center Division, Newport, RI, NUWC-NPT Technical Report 10,590, 11 July 1996.

Keenan, R. E., 2000. An introduction to GRAB eigenrays and CASS reverberation and signal excess. Proceedings on IEEE/MTS Oceans 2000, 6 pages (in CD Rom). 11-14 September 2000, Providence Rhode Island.

Keenan, R. E. and H. Weinberg. 2001. Gaussian ray bundle (GRAB) model shallow water acoustic workshop implementation. J Comput Acoust. 9:133-148.

Kringel, K., P.A. Jumars and D.V. Holiday. 2003. A shallow scattering layer: High-resolution acoustic analysis of nocturnal vertical migration from the seabed. Limnol Oceanogr. 48(3):1223-1234.

Leroy, C.C. 1969. Development of Simple Equations for Accurate and More Realistic Calculation of the Sound Speed in Sea Water. J Acoust Soc Am. 46(1):216-226.

Millero, F.J. and Li, X. 1994. Comments on "On Equations for the Speed of Sound in Seawater". J Acoust Soc Am. 95(5):2757-2759.

Naval Oceanographic Office Systems Integration Division. 1999a. Software Design Document for the Gaussian Ray Bundle (GRAB) Eigenray Propagation Model. OAML-SDD-74. Stennis Space Cneter, MS.

Naval Oceanographic Office Systems Integration Division. 1999b. Software Requirements Specification for the Gaussian Ray Bundle (GRAB) Eigenray Propagation Model. OAML-SRS-74. Stennis Space Center, MS.

Urick, R.J. 1983. Principles of Underwater Sound, McGraw-Hill, New York, 423 pp.

Weinberg, H., and R. E. Keenan. 1996. Gaussian ray bundles for modeling high-frequency propagation loss under shallow water condition. J Acoust SocAm. 100(3):1421-1431.

Wilson, W.D. 1960. Equation for the speed of sound in sea water. J Acoust Soc Am. 32:1357-1367.